

A new numerical method for constructing quasi-equilibrium sequences of irrotational binary neutron stars in general relativity

Kōji Uryū

SISSA, Via Beirut 2/4, Trieste 34013, Italy

International Center for Theoretical Physics, Strada Costiera 11, Trieste 34100, Italy

Yoshiharu Eriguchi

Department of Earth Science and Astronomy, Graduate School of Arts and Sciences, University of Tokyo, Komaba, Meguro, Tokyo 153-8902, Japan

We propose a new numerical method to compute quasi-equilibrium sequences of general relativistic irrotational binary neutron star systems. It is a good approximation for an inspiraling binary neutron star system just before the coalescence as a result of gravitational wave emission that (1) the binary star system is irrotational, i.e. a vorticity of flow field inside component stars vanishes everywhere (irrotational flow), and (2) the binary star system is in quasi-equilibrium. We can introduce the velocity potential for such irrotational flow field, which satisfies an elliptic partial differential equation (PDE) with a Neumann type boundary condition at the stellar surface. For the treatment of general relativistic gravity, we use the Wilson–Mathews formulation, which assumes conformal flatness for spatial components of metric. In this formulation, the basic equations are expressed by a system of elliptic PDEs. We have developed a method to solve these PDEs with appropriate boundary conditions. The method is based on the established prescription to compute equilibrium states of rapidly rotating axisymmetric neutron stars or Newtonian binary systems. We have checked the reliability of our new code by comparing our results with those of other computations available. By using this code, we have obtained quasi-equilibrium sequences of irrotational binary star systems with strong gravity as models for final states of real evolution of binary neutron star systems just before coalescence. Analysis of our quasi-equilibrium sequences of binary star systems shows that the systems may not suffer from dynamical instability of the orbital motion and that the maximum density does not increase substantially.

PACS number(s): 04.25.Dm, 04.30.Db, 04.40.Dg, 97.60.Jd

I. INTRODUCTION

At the beginning of the next century, advanced gravitational wave detectors (LIGO/VIRGO/TAMA/GEO; [1]) will provide us signals from coalescing binary neutron star systems. According as types of compact objects (for example, black holes/neutron stars, isolated/binary objects, solar mass/super massive objects), various theoretical methods have been developed or are under way to predict and interpret gravitational wave signals which will be observed. Compact binary systems of solar mass sizes are also promising sources of γ -ray bursts or r-process nuclei. They are important issues of recent astrophysics (see for example [2] and references therein).

When we consider the final evolutionary stage of the binary neutron star (BNS) as a result of gravitational wave emission, it is necessary to solve the internal structure of the neutron star (NS) at the late inspiraling stage as well as the early stage of merging, since the size of the star is comparable to the separation of two neutron stars. In this case, (1) tidal deformation of a component star, (2) the general relativistic effect on the orbital motion, and (3) the general relativistic effect on the internal structure of a star are coupled to affect the physics of the binary system. Such finite size effects are not negligible at the

last $\mathcal{N} \lesssim 10$ cycles of the inspiraling phase just before coalescence [2].

According to the scenario of the final evolution of the close BNS [3], a flow field inside component stars just prior to coalescence becomes *irrotational*, i.e. a vorticity seen from the non-rotating observer's frame vanishes just prior to coalescence. The irrotational flow is realized because (1) a viscosity of neutron star matter is too weak to synchronize a spin of component stars and an orbital angular velocity of the binary system during the evolution, and (2) the initial spin period of each NS is much larger than the final orbital period of the BNS. It is precisely this stage of the binary evolution that we focus on in the present paper.

Full 3D numerical simulations are most promising to investigate such final phases of BNS systems. Numerical methods for fully dynamical 3D GR computations of BNS's are developing rapidly (see for example [4–6]). However it is still difficult to perform simulations over the whole $\mathcal{N} \lesssim 10$ cycles of the inspiraling BNS because there remain some technical problems to overcome for newly developed 3D GR codes, such as, maintaining stability and accuracy of numerical schemes or computational power of present computers. Recently, Shibata has succeeded in developing a new numerical method to

compute dynamical evolution of the space-time and compact object(s) such as a single NS or a BNS system in a stable manner [6]. Therefore simulations over several orbital periods of BNS will be performed in the near future. However, even after that, it is quite desirable to have totally different and supplemental methods to investigate such systems to test the reliability of the theory based on numerical methods.

One of promising ways to tackle this problem differently is to compute quasi-equilibrium sequences of BNS configurations. Since the time scale of evolution as a result of gravitational wave (GW) emission is longer than the time scale of the orbital motion even at this stage, quasi-equilibrium is a good approximation for a realistic BNS system [7]. Therefore, a quasi-equilibrium sequence with a constant rest mass constructed by changing the binary separation could be considered as an evolutionary sequence of such inspiraling BNS system. Also, quasi-equilibrium configurations give accurate initial conditions for the future 3D GR dynamical computations. Therefore, it is important to develop a numerical method to compute quasi-equilibrium configurations of close BNS's.

In this paper we introduce a new numerical method to compute quasi-equilibrium configurations of irrotational BNS systems. It is a straightforward extension of the computational method for the Newtonian irrotational binary systems developed by the present authors [8]. We discuss the formulation of the problem separately for (1) the gravitation part (Einstein equations) and (2) the fluid part (NS, i.e., the equation of motion, the continuity equation, the equation of state (EOS) and so on). As the first step of the extension to general relativistic strong gravity, a simplified system of the Einstein equations is employed. We use the formulation developed by Wilson and Mathews [9] and Baumgarte et al. [10], in which the metric is decomposed into (3+1) form and its spatial part is assumed to be conformally flat. For the fluid part, we solve the equations for the irrotational flow whose formulation in GR is developed by Shibata [11] and Teukolsky [12] (see also [13]). Our new computational code reproduces results of several independent computations previously made for GR co-rotating BNS's or Newtonian irrotational binary systems with reasonable accuracy. Using this new code, we construct quasi-equilibrium sequences of irrotational BNS's with constant rest mass, which approximate the final evolution track of a realistic BNS as a result of GW emission. Analysis of our quasi-equilibrium sequences of binary star systems suggests that the systems may not suffer from dynamical instability of the orbital motion and that the maximum density does not increase substantially.

This paper is organized as follows. In section II we review the formulation for quasi-equilibrium irrotational binary systems in GR and derive the basic equations. In section III, we present the new numerical method to solve them. In section IV, several comparisons with other computations and numerical results for the binary configurations and quasi-equilibrium sequences are presented.

In section V, we discuss the validity of the present results and the future prospects.

II. REVIEW OF THE FORMULATION OF THE PROBLEM

A. Quasi-equilibrium irrotational binary systems in GR: Summary for the assumptions and the formulation

Because of the finite size effect of stars in a close binary system, it is necessary to solve structures of the stars without approximation for the last $\mathcal{N} \lesssim 10$ cycles of the inspiraling phase just before coalescence. In general, the binary system cannot be in equilibrium in GR since GW carries the angular momentum and the energy away to infinity. However, the quasi-equilibrium approximation is well fulfilled since the time scale of evolution due to GW emission is longer than that of the orbital period even just before coalescence [7]. In this situation, we can expect that (A) there exists an approximate Killing vector $\vec{\ell}$ to express this symmetry of the space-time and the fluid. Moreover, it is pointed out by Kochanek and by Bildsten & Cutler [3] that (B) the flow fields of binary stars just before coalescence become *irrotational*, because (i) the viscosity of the neutron star matter is too weak to synchronize the spin and the orbital angular velocity during the evolution by the time of merging and (ii) the initial spin angular velocity of each component star is negligible compared to the final orbital angular velocity.

To construct realistic BNS's in quasi-equilibrium, the above two properties (A) and (B) should be implemented in the formulation of basic equations. Strictly speaking, it is impossible to assume the property (A) in exact GR, because there arises GW emission from the source to the asymptotically flat region. It implies that there is no unique way to formulate properly an approximation which fulfills the property (A) for the Einstein equations. However, several authors have developed some formulations for BNS's in quasi-equilibrium. The formulation for the first/second post-Newtonian (1PN/2PN, respectively) approximation has been developed and co-rotating quasi-equilibrium configurations of BNS's in the 1PN approximation has been solved [14]. Also, the Wilson–Mathews formulation has been implemented to express quasi-equilibrium BNS's as well as space-time around them by several authors [9,10]. In this paper we use the Wilson–Mathews formulation to express the gravitational field. For the fluid, the property (B) is implemented by introducing the velocity potential and assuming the barotropic flow. The property (A) is imposed by decomposing the variables into the direction of the Killing vector $\vec{\ell}$ and the spatial direction [11–13].

Consequently the basic equations we use in this paper are identical with those used in Bonazzola, Gourgoulhon

and Marck [15] and in Marronetti, Mathews and Wilson [16]. We will summarize the formulation and the basic equations below. The geometrical units $G = 1 = c$ are used throughout this paper. Latin indices will run from 1 to 3, whereas Greek indices will run from 0 to 3.

B. Formulation for the gravitational field

We adopt the ADM decomposition for the convenience of numerical computations. The metric is written as,

$$\begin{aligned} ds^2 &= g_{\mu\nu} dx^\mu dx^\nu \\ &= -\alpha^2 dt^2 + \gamma_{ij} (dx^i - \omega^i dt) (dx^j - \omega^j dt), \end{aligned} \quad (1)$$

where $g_{\mu\nu}$, α , ω^i and γ_{ij} are the 4-metric, the lapse function, the shift vector and the 3-metric on a 3D spatial hypersurface Σ_t , respectively. The unit normal to Σ_t is written as

$$n^\mu = \left(\frac{1}{\alpha}, \frac{\omega^i}{\alpha} \right) \quad \text{and} \quad n_\mu = (-\alpha, 0, 0, 0), \quad (2)$$

and $\gamma_{\mu\nu}$ is defined as

$$\gamma_{\mu\nu} = g_{\mu\nu} + n_\mu n_\nu. \quad (3)$$

By using the (3+1) formalism, the Einstein equations are decomposed into the constraint equations and the evolution equations. The Hamiltonian constraint and the momentum constraints are, respectively,

$$R - K_{ij}K^{ij} + K^2 = 16\pi\rho_H, \quad (4)$$

$$D_j K^{ij} - D^i K = 8\pi j^i, \quad (5)$$

where the source term ρ_H and j^σ are defined by

$$\rho_H = n^\mu n^\nu T_{\mu\nu}, \quad (6)$$

$$j^\sigma = -\gamma^\sigma_\mu n_\nu T^{\mu\nu}. \quad (7)$$

Here R , K_{ij} , K , D_i and $T_{\mu\nu}$ are the scalar curvature, the extrinsic curvature, the trace part of K_{ij} , the covariant derivative with respect to γ_{ij} , and the stress-energy tensor, respectively.

According to the (3+1) formalism, the 3-metric γ_{ij} satisfies the dynamical equations

$$\frac{\partial}{\partial t} \gamma_{ij} = -2\alpha K_{ij} - D_i \omega_j - D_j \omega_i. \quad (8)$$

These equations are decomposed into its trace part and trace free parts [17] :

$$\frac{\partial}{\partial t} \ln \gamma^{1/2} = -\alpha K - D_i \omega^i, \quad (9)$$

$$\begin{aligned} \gamma^{1/3} \frac{\partial}{\partial t} (\gamma^{-1/3} \gamma_{ij}) &= -2\alpha \left(K_{ij} - \frac{1}{3} \gamma_{ij} K \right) \\ &\quad - D_i \omega_j - D_j \omega_i + \frac{2}{3} \gamma_{ij} D_k \omega_k. \end{aligned} \quad (10)$$

where $\gamma = \det \gamma_{ij}$ and $K = K^i_i$.

The dynamical equations for K_{ij} are also derived and decomposed into its trace part and trace free parts. We only write the trace part :

$$\begin{aligned} \frac{\partial K}{\partial t} &= \alpha R - D^i D_i \alpha + \alpha K^2 - \omega^i D_i K \\ &\quad - 4\pi\alpha (3\rho_H - S), \end{aligned} \quad (11)$$

where S is defined as

$$S = \gamma^{ij} T_{ij}. \quad (12)$$

The post-Newtonian approach up to the 2PN order admits exact equilibrium states of BNS's [14]. However, the 2PN equations for gravity require a significant amount of computations. Also, the problem of GR formulation for quasi-equilibrium states has not been settled. To make the problem tractable, we assume that the spatial part of the metric γ_{ij} to be conformally flat for all the time during the inspiraling stage as follows:

$$\gamma^{-1/3} \gamma_{ij} = f_{ij}, \quad (13)$$

$$\gamma_{ij} = \gamma^{1/3} f_{ij} \equiv \Psi^4 f_{ij}. \quad (14)$$

where f_{ij} is the flat space metric and Ψ is a conformal factor [9,10]. Under this assumption, we can compute exactly BNS's up to 1PN order and spherically symmetric configurations in full GR. It is also expected that this choice minimizes the gravitational wave content of the (physical) space-time by removing the dynamical or “wave” degrees of freedom from the field. Moreover, since this choice can always be adopted to find initial data without any approximation, our solutions will give initial conditions for future 3D simulations of BNS coalescence in full GR.

For the time slicing condition we may choose the maximal slicing:

$$K = 0, \quad (15)$$

and we assume that this condition holds for all the time of the evolution

$$\frac{\partial K}{\partial t} = 0, \quad (16)$$

although the other evolution equations for K_{ij} are omitted artificially.

From the above assumptions Eq. (13) – (16), the basic equations for the gravitational field become as follows. The scalar curvature reduces to

$$R = -8\Psi^{-5}\nabla^2\Psi, \quad (17)$$

where $\nabla^2 = \nabla^i \nabla_i = f^{ij} \nabla_i \nabla_j$ is the Laplacian of flat 3-space. Eqs. (4), (5), (10) and (11) are rewritten as

$$\nabla^2\Psi = -\frac{1}{8}\Psi^{-7}\tilde{K}_{ij}\tilde{K}^{ij} - 2\pi\Psi^5\rho_H, \quad (18)$$

$$\nabla^2\omega^i + \frac{1}{3}\nabla^i\nabla_j\omega^j = -2\nabla_j(\alpha\Psi^{-6})\tilde{K}^{ij} - 16\pi\alpha\Psi^4j^i, \quad (19)$$

$$\tilde{K}^{ij} = -\frac{\Psi^6}{\alpha}\left(\frac{1}{2}(\nabla^i\omega^j + \nabla^j\omega^i) - \frac{1}{3}f^{ij}\nabla_k\omega^k\right), \quad (20)$$

$$\nabla^2(\alpha\Psi) = \alpha\Psi\left(\frac{7}{8}\Psi^{-8}\tilde{K}_{ij}\tilde{K}^{ij} + 2\pi\Psi^4(\rho + 2S)\right). \quad (21)$$

Here we define \tilde{K}^{ij} as

$$\tilde{K}^{ij} = \Psi^{10}K^{ij}, \quad (22)$$

and its indices are lowered by the flat metric f_{ij} , as $\tilde{K}_{ij} = f_{ik}f_{jl}\tilde{K}^{kl}$. ∇_i is the derivative with respect to the flat metric f_{ij} .

To make Eq. (19) more tractable, the shift vector ω^i is decomposed as a sum of a vector and a gradient of a scalar as

$$\omega^i = G^i - \frac{1}{4}\nabla^i B. \quad (23)$$

Eq. (19) is divided into the following equations for these variables G^i and B as,

$$\nabla^2 G^i = -2\nabla_j(\alpha\Psi^{-6})\tilde{K}^{ij} - 16\pi\alpha\Psi^4j^i, \quad (24)$$

$$\nabla^2 B = \nabla_i G^i. \quad (25)$$

After all, the basic variables of the gravitational potentials for the actual computation are Ψ , α , G^i and B , and corresponding equations are Eqs. (18), (21), (24) and (25), together with relations (20) and (23). It should be noted that all these equations are the elliptic type PDEs. We can solve these equations with appropriate boundary conditions iteratively by a certain computational method, which is described in the later section.

C. Formulation for the fluid part

General relativistic irrotational flows have been considered as the extension of the Newtonian case and applied for the accretion onto the black hole [18]. The formulation of the irrotational flow for inspiraling BNS's in quasi-equilibrium is derived independently by Shibata

[11] and by Teukolsky [12]. We will follow their formulation.

The energy momentum tensor of the perfect fluid can be written as

$$T_{\mu\nu} = \rho\left(1 + \varepsilon + \frac{P}{\rho}\right)u_\mu u_\nu + Pg_{\mu\nu}, \quad (26)$$

where ρ , ε , P and u_μ are the rest mass density, the specific internal energy, the pressure and the 4-velocity, respectively. We assume the polytropic EOS for the perfect fluid

$$P = (\Gamma - 1)\rho\varepsilon = \kappa\rho^{1+1/n}, \quad (27)$$

where n is the polytropic index, $\Gamma = 1 + 1/n$, and κ is a constant. We define the relativistic specific enthalpy h as

$$h = 1 + \varepsilon + \frac{P}{\rho} = 1 + \kappa(n+1)\rho^{1/n}. \quad (28)$$

The conservation equation for the energy momentum tensor

$${}^{(4)}\nabla_\mu T^\mu_\nu = 0, \quad (29)$$

can be rewritten to Euler's equation

$$u^\mu {}^{(4)}\nabla_\mu(hu_\nu) + {}^{(4)}\nabla_\nu h = 0, \quad (30)$$

where ${}^{(4)}\nabla_\mu$ is the covariant derivative with respect to $g_{\mu\nu}$. The conservation of the rest mass density is written as

$${}^{(4)}\nabla_\mu(\rho u^\mu) = 0. \quad (31)$$

The covariant definition of irrotationality in 4D is

$$\begin{aligned} \omega_{\mu\nu} &= P^\alpha_\mu P^\beta_\nu \left({}^{(4)}\nabla_\beta u_\alpha - {}^{(4)}\nabla_\alpha u_\beta \right) \\ &= \frac{1}{h} \left({}^{(4)}\nabla_\nu(hu_\mu) - {}^{(4)}\nabla_\mu(hu_\nu) \right) = 0, \end{aligned} \quad (32)$$

where $P^\mu_\nu = g^\mu_\nu + u^\mu u_\nu$ is the projection tensor and we have made use of Eq. (30). Thus the quantity hu_μ can be expressed by the gradient of a potential Φ as

$$hu_\mu = {}^{(4)}\nabla_\mu \Phi. \quad (33)$$

We call Φ the velocity potential hereafter. Then the equation of the rest mass conservation (31) is rewritten as

$${}^{(4)}\nabla^\mu {}^{(4)}\nabla_\mu \Phi = - {}^{(4)}\nabla^\mu \left(\ln \frac{\rho}{h} \right) {}^{(4)}\nabla_\mu \Phi. \quad (34)$$

From the normalization condition for the 4-velocity $u_\mu u^\mu = -1$, we get the following equation for h

$$h = \left[- {}^{(4)}\nabla_\mu \Phi {}^{(4)}\nabla^\mu \Phi \right]^{1/2}. \quad (35)$$

This is the generalized Bernoulli's equation in GR since it is also derived by integrating Euler's equation (30) as follows,

$$\begin{aligned} & h \left(u^\mu {}^{(4)}\nabla_\mu (h u_\nu) + {}^{(4)}\nabla_\nu h \right) \\ &= \frac{1}{2} {}^{(4)}\nabla_\nu \left({}^{(4)}\nabla_\mu \Phi {}^{(4)}\nabla^\mu \Phi + h^2 \right) = 0. \end{aligned} \quad (36)$$

Now we decompose Eqs. (34) and (35) into the ADM (3+1) form and impose the quasi-equilibrium condition. The quasi-equilibrium condition is implemented by assuming the existence of a timelike Killing vector ℓ^μ such that

$${}^{(4)}\nabla_\nu \ell_\mu + {}^{(4)}\nabla_\mu \ell_\nu = 0 \quad (37)$$

and

$$\mathcal{L}_\ell f = \ell^\mu {}^{(4)}\nabla_\mu f = 0 \quad (38)$$

where f denotes a certain fluid variable such as ρ , h or u_μ . \mathcal{L}_ℓ denotes the Lie derivative along ℓ^μ . Since we have assumed the polytropic EOS and the irrotational flow, the number of independent fluid variables are two, i.e. the velocity potential Φ and, for example, the density ρ . Note however that not Φ but its gradient is the fluid variable. Therefore, the following relation holds

$$\mathcal{L}_\ell(hu) = \mathcal{L}_\ell(d\Phi) = d(\mathcal{L}_\ell\Phi) = 0, \quad (39)$$

that is,

$$\mathcal{L}_\ell\Phi = \ell^\mu {}^{(4)}\nabla_\mu \Phi = -C \quad (40)$$

where C is a positive 'global' constant on the fluid.

Performing the (3+1) decomposition of Eqs. (34) and (35), and imposing the quasi-equilibrium conditions (38) and (40), we have the following basic equations for irrotational binary systems, respectively [11,12],

$$\begin{aligned} & D^i D_i \Phi - B^i D_i \frac{\lambda}{\alpha^2} - \frac{\lambda K}{\alpha} \\ &= - \left(D^i \Phi - \frac{\lambda}{\alpha^2} B^i \right) D_i \ln \frac{\alpha \rho}{h}, \end{aligned} \quad (41)$$

$$h^2 = \frac{\lambda^2}{\alpha^2} - D_i \Phi D^i \Phi. \quad (42)$$

Here, B^i is a rotating shift vector defined as

$$\ell^\mu = \alpha n^\mu + B^\mu, \quad B^\mu = -\omega^\mu + \Omega \xi^\mu, \quad (43)$$

where ξ^μ is the generator of rotations about the rotation axis of the binary. λ is defined as

$$\lambda = C + B^j D_j \Phi. \quad (44)$$

Using the quasi-equilibrium conditions Eqs. (38) and (40), we obtain the following expressions for normal

derivatives of a scalar quantity f and the velocity potential Φ ,

$$\begin{aligned} n^\mu {}^{(4)}\nabla_\mu f &= \frac{1}{\alpha} (\ell^\mu - B^\mu) {}^{(4)}\nabla_\mu f \\ &= -\frac{1}{\alpha} B^i D_i f, \end{aligned} \quad (45)$$

and

$$\begin{aligned} n^\mu {}^{(4)}\nabla_\mu \Phi &= \frac{1}{\alpha} (\ell^\mu - B^\mu) {}^{(4)}\nabla_\mu \Phi \\ &= -\frac{1}{\alpha} (C + B^i D_i \Phi) = -\frac{\lambda}{\alpha}. \end{aligned} \quad (46)$$

The boundary condition for the equation of the velocity potential is derived from the fact that the spatial fluid velocity on the stellar surface flows along the stellar surface on each 3D spatial hypersurface as follows. We decompose u^μ as

$$u^\mu = u^0 (\ell^\mu + V^\mu). \quad (47)$$

and assume that V^μ is a spatial vector, $n_\mu V^\mu = 0$. By using V^μ , the boundary condition is expressed as

$$V^i D_i \rho|_{\text{surf}} = 0. \quad (48)$$

From the definition for V^μ , we obtain

$$\begin{aligned} n_\mu V^\mu &= \frac{1}{u^0} n_\mu u^\mu - n_\mu \ell^\mu \\ &= \frac{1}{u^0} \left(-\frac{\lambda}{\alpha h} \right) + \alpha = 0. \end{aligned} \quad (49)$$

Therefore V^μ is rewritten as follows.

$$\begin{aligned} V^\mu &= \gamma^\mu_\nu V^\nu \\ &= \frac{1}{u^0} \gamma^\mu_\nu u^\nu - \gamma^\mu_\nu \ell^\nu \\ &= \frac{\alpha^2}{\lambda} \left(D^\mu \Phi - \frac{\lambda}{\alpha^2} B^\mu \right), \end{aligned} \quad (50)$$

where Eqs. (43), (46) and (49) are used. From this expression, the boundary condition (48) is written as

$$\left(D^i \Phi - \frac{\lambda}{\alpha^2} B^i \right) D_i \rho \Big|_{\text{surf}} = 0. \quad (51)$$

This is identical with the one derived from imposing the finiteness of r.h.s. of Eq. (41) on the compact support of a star which assures that the elliptic PDE for Φ is well-defined on it.

Finally, we impose the spatially conformal flatness Eq. (14) and the maximal slicing condition Eq. (15). By using the following identities for the derivative of a scalar function,

$$D^i D_i \Phi = \Psi^{-4} \nabla^2 \Phi + 2\Psi^{-5} \nabla^i \Psi \nabla_i \Phi, \quad (52)$$

$$D_i A = \nabla_i A \quad \text{and} \quad D^i A D_i B = \Psi^{-4} \nabla^i A \nabla_i B, \quad (53)$$

basic equations and boundary conditions for the fluid part, namely, Eqs. (41), (42), and (51) are rewritten as follows,

$$\begin{aligned} \nabla^i \nabla_i \Phi = & -\frac{2}{\Psi} \nabla^i \Psi \nabla_i \Phi + \Psi^4 B^i \nabla_i \frac{\lambda}{\alpha^2} \\ & - \left(\nabla^i \Phi - \frac{\lambda}{\alpha^2} \Psi^4 B^i \right) \nabla_i \ln \frac{\alpha \rho}{h}, \end{aligned} \quad (54)$$

$$h^2 = \frac{\lambda^2}{\alpha^2} - \Psi^{-4} \nabla_i \Phi \nabla^i \Phi, \quad (55)$$

and

$$\left(\nabla^i \Phi - \frac{\lambda}{\alpha^2} \Psi^4 B^i \right) \nabla_i \rho \Big|_{\text{surf}} = 0, \quad (56)$$

where ,

$$\lambda = C + B^j \nabla_j \Phi, \quad B^i = \Omega \xi^i - \omega^i. \quad (57)$$

We also need another boundary condition to determine the stellar surface. It comes from the definition of the surface itself,

$$P = 0. \quad (58)$$

Eqs. (54) and (56) form a system of the elliptic type PDE with the Neumann boundary condition .

Now we derive the matter source terms which appear in the Einstein equations, i.e. ρ_H , j^σ and S . From definitions,

$$\rho_H = n^\mu n^\nu T_{\mu\nu} = \frac{\rho \lambda^2}{h \alpha^2} - P, \quad (59)$$

$$S = \gamma^{\mu\nu} T_{\mu\nu} = \frac{\rho \lambda^2}{h \alpha^2} - \rho h + 3P, \quad (60)$$

$$j^i = -\gamma^{i\mu} n^\nu T_{\mu\nu} = \frac{\rho \lambda}{h \alpha} D^i \Phi = \frac{\rho \lambda}{h \alpha} \Psi^{-4} \nabla^i \Phi. \quad (61)$$

III. COMPUTATIONAL METHOD FOR IRROTATIONAL BINARY SYSTEMS IN GR

In this section, we describe the solving method for the basic equations derived in the previous section. This is essentially the extension of the method developed by the authors and co-workers and successfully applied to solve the structure of a rapidly rotating single star, or a binary system in Newtonian gravity or in GR [8,19,20].

| | $\theta_g = \pi/2$ | $\varphi_g = 0$ | $\varphi_g = \pi/2$ | $r_g \rightarrow \infty$ |
|--------------------------|--------------------|-----------------|---------------------|---|
| Ψ | sym | sym | sym | $1 + \mathcal{O}\left(\frac{1}{r}\right)$ |
| α | sym | sym | sym | $1 + \mathcal{O}\left(\frac{1}{r}\right)$ |
| G^r | sym | anti-sym | anti-sym | $\mathcal{O}\left(\frac{1}{r^2}\right)$ |
| G^θ | anti-sym | anti-sym | anti-sym | $\mathcal{O}\left(\frac{1}{r^2}\right)$ |
| G^φ | sym | sym | sym | $\mathcal{O}\left(\frac{1}{r^2}\right)$ |
| $\sin \varphi G^\varphi$ | sym | anti-sym | sym | $\mathcal{O}\left(\frac{1}{r^2}\right)$ |
| B | sym | anti-sym | anti-sym | $\mathcal{O}\left(\frac{1}{r}\right)$ |
| | $\theta_f = \pi/2$ | $\varphi_f = 0$ | $\varphi_f = \pi$ | $r_f = R_S$ |
| ρ | sym | sym | sym | Eq. (58) |
| Φ | sym | anti-sym | anti-sym | Eq. (56) |

TABLE I. Symmetries of variables and their boundary conditions are listed. ‘sym’ and ‘anti-sym’ denote plane symmetry and anti-symmetry, respectively. Boundary conditions at the outer boundaries, i.e. $r_g \rightarrow \infty$ for the gravitational potentials and $r_f = R_S$ for the fluid, where R_S is the stellar surface. The equatorial plane is taken to be the $\theta = \pi/2$ plane and the stars are located aligned along the $(\theta_g, \varphi_g) = (\pi/2, 0)$ -axis.

A. Coordinates and symmetries

For the actual computation, we prepare two spherical coordinate systems, one for the gravitational field whose origin is at the intersection of the rotational axis and the equatorial plane, and the other for the fluid variables whose origin is at the coordinate center of the star. We will call them as the gravitational coordinates and the fluid coordinates, respectively. In case of need, we will distinguish these two coordinates by subscripts g and f as $(r_g, \theta_g, \varphi_g)$ and $(r_f, \theta_f, \varphi_f)$, respectively.

We assume the symmetry of the physical quantities as shown in Table I. Note that the equatorial plane of the star is the $\theta_g = \pi/2 = \theta_f$ plane and the axis of orbital motion is located at $\theta_g = 0$. Planes of (anti-)symmetry are the equatorial plane and a plane with $\varphi_g = 0$ for the gravitational coordinates, $\varphi_f = 0$ and $\varphi_f = \pi$ for the fluid coordinates. In this paper, we only consider an equal mass BNS system and hence a plane of (anti-)symmetry with respect to $\varphi_g = \pi/2$ exists for the gravitational coordinates as well.

Because of these symmetries, we only need to treat one octant of the spherical coordinate system for the gravitation, namely, $(r_g, \theta_g, \varphi_g) \in [0, \infty) \times [0, \pi/2] \times [0, \pi/2]$. For the fluid coordinate system, we need to treat a quarter of the whole star, that is, $(r_f, \theta_f, \varphi_f) \in [0, R] \times [0, \pi/2] \times [0, \pi]$, where R is the largest coordinate radius of the star

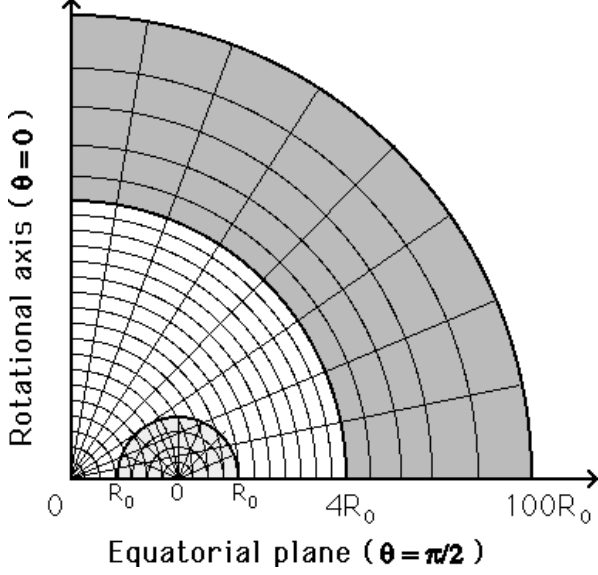


FIG. 1. Schematic figure of the coordinate systems used in the actual computation. A larger spherical coordinate system corresponds to that for gravitation (white and dark gray region). A smaller spherical coordinate system corresponds to that for the fluid (gray region). R_0 is defined as $R_0 = (R_{\text{out}} - R_{\text{in}})/2$.

in the fluid spherical coordinates. We set the coordinate center of the star to be at $(r_g, \theta_g, \varphi_g) = (d, \pi/2, 0)$ of the gravitational coordinate system, where

$$d = (R_{\text{out}} + R_{\text{in}})/2, \quad (62)$$

is defined as the coordinate center of the star, and $(r_g, \theta_g, \varphi_g) = (R_{\text{out}}, \pi/2, 0)$ and $(r_g, \theta_g, \varphi_g) = (R_{\text{in}}, \pi/2, 0)$ are the outer and inner edges of the star, respectively. We show a schematic figure of the coordinate systems in Figure 1.

Since we have assumed conformal flatness in space, we may introduce these spherical coordinate systems in the same manner as we do for Newtonian models. Especially, since the derivatives appearing in basic equations are that for flat 3-metric f_{ij} , it is convenient to take non-coordinate basis whose metric becomes the unit matrix $f_{ij} = \delta_{ij} = \text{diag}(1, 1, 1)$ as is usually done for the vector analysis in the flat space, where δ_{ij} is the Kronecker delta. We write the orthonormal non-coordinate basis for the spherical coordinates as

$$\{\mathbf{e}_r, \mathbf{e}_\theta, \mathbf{e}_\varphi\}, \quad \text{where} \\ \mathbf{e}_a \cdot \mathbf{e}_b = \delta_{ab}, \quad (a, b = r, \theta, \varphi). \quad (63)$$

In case of need, we will distinguish the bases for the gravitational coordinate system and the fluid coordinate system by prescript g and f , respectively. By using these bases, the gradient of a scalar function ϕ is written as

$$\nabla^i \phi = \nabla_i \phi = \mathbf{e}_r \frac{\partial \phi}{\partial r} + \mathbf{e}_\theta \frac{1}{r} \frac{\partial \phi}{\partial \theta} + \mathbf{e}_\varphi \frac{1}{r \sin \theta} \frac{\partial \phi}{\partial \varphi}. \quad (64)$$

Hereafter, we often make use of the index notation and the notation of vector analysis in the same equation as above for convenience.

B. Poisson solver

Seven elliptic type PDEs appear in our formulation. They are Eqs. (18), (21), (24) and (25) for the gravitational field, and Eq. (54) for the fluid variable. To solve these equations, firstly, the flat part of 3D Laplacian is separated out. Then, the equations are transformed into integral forms by using Green's function of 3D Laplacian.

$$\Delta \phi_{(a)} = S_{(a)}. \quad (65)$$

Here the suffix (a) is an index to specify each equation, and Δ is the 3D flat Laplacian in the spherical coordinates,

$$\Delta \phi_{(a)} = \frac{1}{r^2} \frac{\partial}{\partial r} \left(r^2 \frac{\partial \phi_{(a)}}{\partial r} \right) + \frac{1}{r \sin \theta} \frac{\partial}{\partial \theta} \left(\sin \theta \frac{\partial \phi_{(a)}}{\partial \theta} \right) + \frac{1}{r^2 \sin^2 \theta} \frac{\partial^2 \phi_{(a)}}{\partial \varphi^2}. \quad (66)$$

By using Green's function which satisfies the following equation

$$\Delta \left(-\frac{1}{4\pi} \frac{1}{|\mathbf{r} - \mathbf{r}'|} \right) = \delta(\mathbf{r} - \mathbf{r}'), \quad (67)$$

Eq. (65) is transformed as

$$\phi_{(a)} = -\frac{1}{4\pi} \int \frac{S_{(a)}}{|\mathbf{r} - \mathbf{r}'|} dV' + \chi, \quad (68)$$

where χ is either a function or a constant depending on the boundary condition. We use the Legendre expansion to compute the integral in Eq. (68),

$$\frac{1}{|\mathbf{r} - \mathbf{r}'|} = \sum_{n=0}^{\infty} f_n(r, r') \sum_{m=0}^n \epsilon_m \frac{(n-m)!}{(n+m)!} \\ \times P_n^m(\cos \theta) P_n^m(\cos \theta') \cos m(\varphi - \varphi'), \quad (69)$$

where $f_n(r, r')$ is defined as,

$$f_n(r, r') = \begin{cases} \frac{1}{r} \left(\frac{r'}{r} \right)^n, & \text{for } r' \leq r, \\ \frac{1}{r'} \left(\frac{r}{r'} \right)^n, & \text{for } r \leq r', \end{cases} \quad (70)$$

ϵ_m is defined as,

$$\epsilon_m = \begin{cases} 1, & \text{for } m = 0, \\ 2, & \text{for } m = 1, 2, \dots, n, \end{cases} \quad (71)$$

and $P_n^m(\cos \theta)$ is the associated Legendre function. Here $dV' = r'^2 \sin \theta' dr' d\theta' d\varphi'$.

Eq. (68) is a formal solution in a sense that each source term $S_{(a)}$ contains variables $\{\phi_{(a)}\}$ themselves. Therefore, an iterative method is used to find a solution. All the equations are consistently solved by the self-consistent-field (SCF) iteration scheme [19–21], whose procedure is described in detail in Paper I of [8].

C. Solving method for the gravitational field

To apply the above procedure, we need to separate out the 3D flat Laplacian Δ for the spherical coordinates as in Eq. (66). We may regard ∇^2 operating on scalar valued functions, as in Eqs. (18), (21) and (25), as Δ in Eq. (66). On the other hand, the Laplacian ∇^2 operates on a vector valued function in the l.h.s. of Eq. (24). Although it is possible to use Green's function of the Laplacian for a vector valued function, instead, we explicitly write down its component and derive the form of Eq. (66) in each expression, so that we can follow the same procedure as for the scalars.

In the gravitational coordinates, this procedure goes as follows,

$$\nabla^2 G^j = \nabla^i \nabla_i G^j = \Delta (G^r \mathbf{e}_r^j + G^\theta \mathbf{e}_\theta^j + G^\varphi \mathbf{e}_\varphi^j), \quad (72)$$

$$\begin{aligned} [\nabla^2 G^j]^r &= \mathbf{e}_r \cdot \Delta (G^r \mathbf{e}_r^j + G^\theta \mathbf{e}_\theta^j + G^\varphi \mathbf{e}_\varphi^j) \\ &= \Delta G^r - \frac{2}{r^2} \left(G^r + \frac{G^\theta}{\tan \theta} + \frac{1}{\sin \theta} \frac{\partial G^\varphi}{\partial \varphi} + \frac{\partial G^\theta}{\partial \theta} \right), \end{aligned} \quad (73)$$

$$\begin{aligned} [\nabla^2 G^j]^\theta &= \mathbf{e}_\theta \cdot \Delta (G^r \mathbf{e}_r^j + G^\theta \mathbf{e}_\theta^j + G^\varphi \mathbf{e}_\varphi^j) \\ &= \Delta G^\theta - \frac{2}{r^2} \left(\frac{G^\theta}{2 \sin^2 \theta} + \frac{\cos \theta}{\sin^2 \theta} \frac{\partial G^\varphi}{\partial \varphi} - \frac{\partial G^r}{\partial \theta} \right), \end{aligned} \quad (74)$$

$$\begin{aligned} [\nabla^2 G^j]^\varphi &= \mathbf{e}_\varphi \cdot \Delta (G^r \mathbf{e}_r^j + G^\theta \mathbf{e}_\theta^j + G^\varphi \mathbf{e}_\varphi^j) \\ &= \Delta G^\varphi - \frac{2}{r^2} \left(\frac{G^\varphi}{2 \sin^2 \theta} - \frac{1}{\sin \theta} \frac{\partial G^r}{\partial \varphi} - \frac{\cos \theta}{\sin^2 \theta} \frac{\partial G^\theta}{\partial \varphi} \right), \end{aligned} \quad (75)$$

where Eqs. (73) ~ (75) are the l.h.s. of Eq. (24). For the φ component of Eq. (24), we multiply $\sin \varphi$ and rearrange the terms of Eq. (75) as follows:

$$\begin{aligned} \sin \varphi [\nabla^2 G^j]^\varphi &= \sin \varphi \mathbf{e}_\varphi \cdot \Delta (G^r \mathbf{e}_r^j + G^\theta \mathbf{e}_\theta^j + G^\varphi \mathbf{e}_\varphi^j) \\ &= \Delta (\sin \varphi G^\varphi) - \frac{2}{r^2 \sin^2 \theta} \left(-\sin \theta \sin \varphi \frac{\partial G^r}{\partial \varphi} \right. \\ &\quad \left. - \cos \theta \sin \varphi \frac{\partial G^\theta}{\partial \varphi} - \cos \varphi \frac{\partial G^\varphi}{\partial \varphi} \right). \end{aligned} \quad (76)$$

In these expressions we suppress the subscript g for the gravitational coordinates.

Terms appearing in expressions (73), (74) and (76) in addition to the flat 3D Laplacian Δ are transferred to r.h.s. and are included as a part of the source term of each component. By the above rearrangement, all the basic equations for the gravitational part have been written in the form of Eq. (65). Therefore, we can follow the procedure described in subsection III B. As we show in Table I, the boundary conditions are imposed by setting $\chi = 1$ for Eqs. (18) and (21) and $\chi = 0$ for Eqs. (24) and (25). Because of the symmetries for variables shown in Table I, source terms have corresponding symmetries as well. As a result, appropriate behaviors of integral terms in Eq. (68) at $r \rightarrow \infty$ are automatically satisfied.

D. Solving method for the fluid part

Basic equations and boundary conditions for the fluid part are Eqs. (54) – (58). Since these equations are essentially the same as those of the Newtonian case solved in Paper I, we can apply all the computational techniques developed in that paper. As we mentioned in subsection III A, we prepare the spherical coordinate system to compute the structure of the star whose origin is at the coordinate center of the star. The elliptic type PDE Eq. (54) is solved in this coordinate system by using the same procedure as in subsection III B. Eq. (54) is the form of Eq. (65) and is integrated to Eq. (68). To impose the boundary condition Eq. (56), we regard the term χ in Eq. (68) as a regular homogeneous solution to the Laplace equation inside the star, i.e.,

$$\Delta \chi(r_f, \theta_f, \varphi_f) = 0. \quad (77)$$

In the spherical coordinates, such a homogeneous solutions to Eq. (77) can be expressed by using the associated Legendre functions as follows:

$$\begin{aligned} \chi(r_f, \theta_f, \varphi_f) &= \sum_{l=1}^{\infty} \sum_{m=1}^l a_{lm} r_f^l [1 + (-1)^{l+m}] \\ &\times \left(\frac{(2l+1)(l-m)!}{4\pi(l+m)!} \right)^{1/2} P_l^m(\cos \theta_f) \sin m\varphi_f, \end{aligned} \quad (78)$$

where a_{lm} 's are certain constants. Here we have taken into account the regularity of the solutions at $r_f = 0$ and the symmetry listed in Table I. Coefficients a_{lm} are computed so that the velocity potential Φ satisfies the boundary condition (56).

Eq. (55) is used to compute the density distribution of the star. For numerical computations, we introduce a function q which is similar to the Emden function of Newtonian polytropes defined as follows:

$$q = \frac{P}{\rho}. \quad (79)$$

In terms of this function, we can express

$$\rho = \kappa^{-n} q^n, \quad (80)$$

$$P = \kappa^{-n} q^{n+1}, \quad (81)$$

$$h = 1 + (n+1)q. \quad (82)$$

Substituting the last three expressions into Eq. (55), we find

$$q = \frac{1}{n+1} \left[\left(\frac{\lambda^2}{\alpha^2} - \Psi^{-4} \nabla_i \Phi \nabla^i \Phi \right)^{1/2} - 1 \right]. \quad (83)$$

Accordingly, the matter source terms Eqs. (59)–(61) are rewritten as follows,

$$\rho_H = \kappa^{-n} q^n \left(\frac{\lambda^2}{(1+(n+1)q)\alpha^2} - q \right), \quad (84)$$

$$\begin{aligned} \rho_H + 2S &= \kappa^{-n} q^n \\ &\times \left(\frac{3\lambda^2}{(1+(n+1)q)\alpha^2} - (2+(2n-3)q) \right), \end{aligned} \quad (85)$$

$$j^i = \kappa^{-n} q^n \frac{\lambda}{(1+(n+1)q)\alpha} \Psi^{-4} \nabla^i \Phi. \quad (86)$$

For the numerical computation of the fluid part, it is convenient to introduce the surface fitted spherical coordinate system as is used in the Newtonian case [8]. The surface of one NS in the binary system can be expressed by a function $R_S(\theta_f, \varphi_f)$ even when the deformation of the shape is relatively large. By using this function, the new coordinates $(r_f^*, \theta_f^*, \varphi_f^*)$ are defined as follows,

$$r_f^* = \frac{r_f}{R_S(\theta_f, \varphi_f)}, \quad \theta_f^* = \theta_f, \quad \text{and} \quad \varphi_f^* = \varphi_f. \quad (87)$$

The stellar interior with the assumed symmetry is mapped into the region $(r_f^*, \theta_f^*, \varphi_f^*) \in [0, 1] \times [0, \pi/2] \times [0, \pi]$. The surface fitted coordinate is advantageous for computing numerical derivatives and imposing boundary conditions at the stellar surface. Implementation of this coordinate system is described in Paper I in detail.

E. Normalization of quantities and choice of parameters

Non-dimensionalization of variables and proper choices of parameters are important for the iteration scheme to obtain converged equilibrium configurations stably. Since we take the geometrical units $G = 1 = c$, the physical dimensions enter only through the constant κ in the polytropic EOS Eq. (27). In particular, $\kappa^{n/2}$ has a dimension of length. For the convenience of numerical computations, we rescale the coordinate length so that the coordinate radius of the star at the intersection of the

surface and the coordinate line with $(\theta_g, \varphi_g) = (\pi/2, 0)$ to be unity, namely, we introduce a parameter R_0 so that $R_S(\pi/2, 0)/R_0 = 1 = R_S(\pi/2, \pi)/R_0$ in the fluid coordinates.

By using this R_0 , basic equations for the gravitational potentials, Eqs. (18), (21), (24) and (25), whose forms are essentially the same as Eq. (65) or Eq. (68), become as follows,

$$\hat{\Delta} \phi_{(a)} = \hat{S}_{(a)}^g + \kappa^{-n} R_0^2 \hat{S}_{(a)}^m, \quad (88)$$

$$\phi_{(a)} = \chi - \frac{1}{4\pi} \int \frac{\hat{S}_{(a)}^g + \kappa^{-n} R_0^2 \hat{S}_{(a)}^m}{|\hat{\mathbf{r}} - \hat{\mathbf{r}}'|} d\hat{V}', \quad (89)$$

where $\hat{\Delta} = R_0^2 \Delta$. Here $\hat{S}_{(a)}^m$ stands for the non-dimensionalized part of the matter source terms corresponding to Eqs. (59)–(61) or (84)–(86) and $\hat{S}_{(a)}^g$ denote remaining terms. We explicitly show the dependence of those quantities on parameters κ and R_0 . In the equations for the fluid part, κ and R_0 are canceled out after rescaling and non-dimensionalization. By this rescaling, the coordinates and variables are transformed as follows,

$$\begin{aligned} \hat{r} &= \frac{r}{R_0}, \quad \hat{\nabla}_i = R_0 \nabla_i, \quad \hat{\xi}^i = \frac{\xi^i}{R_0}, \quad \hat{R}_S = \frac{R_S}{R_0}, \\ \hat{K}_{ij} &= \tilde{K}_{ij} R_0, \quad \hat{B} = \frac{B}{R_0}, \quad \hat{\Phi} = \frac{\Phi}{R_0}, \quad \hat{\Omega} = \Omega R_0. \end{aligned} \quad (90)$$

We

may consider that κ is used for non-dimensionalization of the variables, and R_0 for rescaling of numerical computations. However, since these two parameters appear in the equations only through the following combination:

$$\bar{R}_0 = \kappa^{-n/2} R_0, \quad (91)$$

we can regard it as one parameter when we compute one solution. In this paper, we only consider $\kappa = \text{const}$ sequences, which could be appropriate for investigation of the final inspiraling stage of BNS's. (In case of constructing solutions, we could mimic physical effect such as heating by changing the value of κ .)

After all, we have three parameters \bar{R}_0 , $\hat{\Omega}$ and C in the basic equations. We need to impose three more conditions to specify them. For this purpose, we choose three locations where q have definite values. Namely, we set $q = 0$ at the intersections of the surface and the coordinate line with $(\theta_g, \varphi_g) = (\pi/2, 0)$, i.e. at two points $(r_f^*, \theta_f^*, \varphi_f^*) = (1, \pi/2, 0)$ and $(1, \pi/2, \pi)$ and also set $q = q_c$ at a grid point where q takes the largest value inside the star [22]. Since we have introduced the surface $\hat{R}_S(\theta_f^*, \varphi_f^*)$ in the surface fitted coordinates, the former two conditions are explicitly imposed by setting $\hat{R}_S(\pi/2, 0) = 1 = \hat{R}_S(\pi/2, \pi)$.

The above three conditions are applied to Eq. (55) at three points to get equations for \bar{R}_0 , $\hat{\Omega}$ and C . It is known [20, 10] that α and Ψ is scaled as

$$\alpha = \hat{\alpha}^{\bar{R}_0^2}, \quad \Psi = \hat{\Psi}^{\bar{R}_0^2/2}. \quad (92)$$

By using this rescaling, Eq. (55) is written as,

$$\hat{\alpha}^{2\bar{R}_0^2} \{1 + (n+1)q\}^2 + \left(\hat{\alpha}\hat{\Psi}\right)^{2\bar{R}_0^2} \hat{\nabla}_i \hat{\Phi} \hat{\nabla}^i \hat{\Phi} - \left\{C + \left(\hat{\Omega}\hat{\xi}^i - \omega^i\right) \hat{\nabla}_i \hat{\Phi}\right\}^2 = 0. \quad (93)$$

We prepare three equations which are derived by imposing the above three conditions at three points in the star, namely, at the inner and outer edges and at the coordinate center of the star. These three non-linear algebraic equations with respect to \bar{R}_0 , $\hat{\Omega}$ and C are solved by using the Newton-Raphson method and their values are updated through the iteration procedure.

The above choice is known to make the iteration converge stably. This choice of parameters and the computation scheme for them are essentially the same as those for rotating single stars [20] or those for co-rotating BNS's [10] in GR.

F. Discretization and numerical computation

Since we have rescaled the length by R_0 , the computational domain is measured by this unit. For the gravitational coordinate system, the whole computational domain is taken as $(\hat{r}_g, \theta_g, \varphi_g) \in [0, \hat{R}_{g,\max}] \times [0, \pi/2] \times [0, \pi/2]$. It is discretized equidistantly for θ_g and φ_g directions. For \hat{r}_g direction, we divide the region into two parts as $[0, \hat{R}_{g,\text{mid}}]$ (white region in Figure 1) and $[\hat{R}_{g,\text{mid}}, \hat{R}_{g,\max}]$ (dark gray region in Figure 1). We discretize the region $[0, \hat{R}_{g,\text{mid}}]$ equidistantly, and the region $[\hat{R}_{g,\text{mid}}, \hat{R}_{g,\max}]$ non-equidistantly. By denoting grid points as $(\hat{r}_i, \theta_j, \varphi_k)$, in which we suppress subscript g , discretization becomes as follows,

$$\hat{r}_{i+1} - \hat{r}_i = \frac{\hat{R}_{g,\text{mid}}}{N_{g,\text{mid}}^r}, \quad \text{where} \quad (94)$$

$$0 \leq \hat{r}_j \leq \hat{R}_{g,\text{mid}}, \quad (0 \leq j \leq N_{g,\text{mid}}^r),$$

$$\hat{r}_{i+1} - \hat{r}_i = \delta(\hat{r}_i - \hat{r}_{i-1}), \quad \text{where}$$

$$\hat{R}_{g,\text{mid}} \leq \hat{r}_j \leq \hat{R}_{g,\max}, \quad (N_{g,\text{mid}}^r \leq j \leq N_{g,\max}^r), \quad (95)$$

$$\theta_{i+1} - \theta_i = \frac{\pi/2}{N_g^\theta}, \quad \text{where}$$

$$0 \leq \theta_j \leq \frac{\pi}{2}, \quad (0 \leq j \leq N_g^\theta), \quad (96)$$

$$\varphi_{i+1} - \varphi_i = \frac{\pi/2}{N_g^\varphi}, \quad \text{where}$$

$$0 \leq \varphi_j \leq \frac{\pi}{2}, \quad (0 \leq j \leq N_g^\varphi). \quad (97)$$

In Eq. (95), $\delta(> 1)$ is a certain constant.

Strictly speaking, $\hat{R}_{g,\max}$ should be infinite to impose the asymptotically flatness as a boundary condition. This could be implemented by using a certain appropriate coordinate transformation to compactify an infinite region which has been used by several authors [23,24]. Although this is straightforward, we do not implement such a special treatment for simplification in the present numerical code. Instead of that we truncate the computational domain at large $\hat{R}_{g,\max}$. It is known that such truncation does not affect the local properties of space-time nor the structure of a single NS and so on [25]. We take rather larger values for $\hat{R}_{g,\max}$.

In the present computation, we typically took following values : $\hat{R}_{g,\text{mid}} = 4$, $\hat{R}_{g,\max} = 100$, $N_{g,\text{mid}}^r = 80$, $N_{g,\max}^r = 100$, $N_g^\theta = 40$ and $N_g^\varphi = 40$. Therefore, a finer mesh is used for the region $[0, \hat{R}_{g,\text{mid}}]$ whose size in \hat{r}_g direction is about twice of the diameter of one NS. The region $[\hat{R}_{g,\text{mid}}, \hat{R}_{g,\max}]$ is discretized into 20 grid points in \hat{r}_g direction. We also truncated the order of Legendre expansion in Eq. (69) up to $0 \leq n \leq 18$ instead of infinity.

For the surface fitted fluid coordinate system, they are discretized equidistantly in all directions as follows,

$$r_{i+1}^* - r_i^* = \frac{1}{N_f^r}, \quad \text{where} \quad (98)$$

$$0 \leq \hat{r}_j^* \leq 1, \quad (0 \leq j \leq N_f^r)$$

$$\theta_{i+1}^* - \theta_i^* = \frac{\pi/2}{N_f^\theta}, \quad \text{where} \quad (99)$$

$$0 \leq \theta_j^* \leq \frac{\pi}{2}, \quad (0 \leq j \leq N_f^\theta),$$

$$\varphi_{i+1}^* - \varphi_i^* = \frac{\pi}{N_f^\varphi}, \quad \text{where} \quad (100)$$

$$0 \leq \varphi_j^* \leq \pi, \quad (0 \leq j \leq N_f^\varphi).$$

In the actual computation, we typically chose the grid numbers as, $N_f^r = 20$, $N_f^\theta = 40$ and $N_f^\varphi = 24$. We also truncated the order of expansion in Eq. (78) up to $0 \leq l \leq 12$ instead of infinity.

As was mentioned before, the basic equations are solved iteratively. The iteration procedure is the same as that for Newtonian irrotational BNS models described in Paper I. Only difference in the numerical scheme is that interpolation of physical quantities from one coordinate system to the other is required. We implemented the cubic spline interpolation method for all directions of the coordinates. The fluid coordinate system is always set inside of the region $[0, \hat{R}_{g,\text{mid}}]$ of the gravitational coordinate system to keep accuracy.

In our formulation, one quasi-equilibrium configuration is specified by three parameters, namely, the half of

separation between the coordinate centers of two component stars \hat{d} , a largest value of q_c on the discretized grid, and the polytropic index n . (Note that κ has been scaled out.) The initial guess for the numerical iteration may be, for instance, an analytic solution of a Newtonian spherical polytrope with $n = 1$ at larger separation, say $\hat{d} = 2$. We started iteration by setting q_c to be small value and could follow iteration cycles. We regarded that the obtained solution is a converged one when relative differences of physical variables of subsequent iterations on each coordinate grid point are less than a certain small value, typically we choose 10^{-5} . Once we get a converged solution, we can change values of parameters by a few tenth of percent. Typically, a solution is converged after $120 \sim 300$ iteration cycles. It takes about 1 minute for one iteration cycle by using DEC Alpha-station 1/166.

IV. NUMERICAL RESULTS FOR IRROTATIONAL BINARY SYSTEMS IN GR

A. Integrals

In this section we show several integral quantities of the equilibrium configurations. The total rest-mass energy $M_{0,\text{tot}}$ of two component stars is defined as

$$M_{0,\text{tot}} = \int_{\mathcal{M}} \rho u^\mu d\Sigma_\mu = \int_{\mathcal{M}} \rho u^\mu (-n_\mu \sqrt{\gamma}) dV, \quad (101)$$

where \mathcal{M} denotes the integration region of the support of two component stars. The non-dimensional form of the total rest-mass can be written by using Eq. (90) and (91) as

$$\begin{aligned} \bar{M}_{0,\text{tot}} &= \kappa^{-n/2} M_{0,\text{tot}} = \kappa^{-n/2} \bar{R}_0^3 \int_{\mathcal{M}} \kappa^{-n} q^n \frac{\lambda}{h\alpha} \Psi^6 d\hat{V} \\ &= \bar{R}_0^3 \int_{\mathcal{M}} \frac{q^n \lambda \Psi^6}{h\alpha} d\hat{V}. \end{aligned} \quad (102)$$

where $d\hat{V} = dV/\bar{R}_0^3$. The total mass-energy (ADM mass) is

$$\begin{aligned} M_{\text{ADM}} &= -\frac{1}{2\pi} \oint_{\infty} \nabla^i \Psi d^2 S_i = -\frac{1}{2\pi} \int_{\infty} \nabla^2 \Psi dV, \\ &= \frac{1}{16\pi} \int_{\infty} \Psi^{-7} \tilde{K}_{ij} \tilde{K}^{ij} dV + \int_{\mathcal{M}} \Psi^5 \rho_H dV \end{aligned} \quad (103)$$

where Eq. (18) derived from the Hamiltonian constraint is used. This can be rewritten in the non-dimensional form as,

$$\begin{aligned} \bar{M}_{\text{ADM}} &= \kappa^{-n/2} M_{\text{ADM}} = \frac{\bar{R}_0}{16\pi} \int_{\infty} \Psi^{-7} \hat{K}_{ij} \hat{K}^{ij} d\hat{V} \\ &\quad + \bar{R}_0^3 \int_{\mathcal{M}} \Psi^5 q^n \left(\frac{\lambda^2}{h\alpha^2} - q \right) d\hat{V}. \end{aligned} \quad (104)$$

The angular momentum is aligned with the $\theta_g = 0$ axis and can be defined as (see, e.g., [26])

$$\begin{aligned} J_{\text{tot}} &= \frac{1}{8\pi} \oint_{\infty} f_{ij} \xi^i \tilde{K}^{jk} d^2 S_k = \frac{1}{8\pi} \int_{\infty} f_{ij} \xi^i \nabla_k \tilde{K}^{jk} dV \\ &= \int_{\mathcal{M}} \Psi^{10} f_{ij} \xi^i j^j dV = \int_{\mathcal{M}} \Psi^{10} r_g \sin \theta_g j^\varphi dV, \end{aligned} \quad (105)$$

where we used $\nabla_k \tilde{K}^{jk} = \Psi^{10} D_k K^{jk}$ as well as the momentum constraints (5), and $\xi = r_g \sin \theta_g \mathbf{e}_\varphi^g$ by definition. This is the total angular momentum contained in the space-time including both the orbital and spin angular momentum of the stars. Finally, we can substitute Eq. (86) for j^i and write the angular momentum in the non-dimensional form

$$\begin{aligned} \bar{J}_{\text{tot}} &= \kappa^{-n} J_{\text{tot}} = \bar{R}_0^4 \int_{\mathcal{M}} \Psi^{10} \hat{r}_g \sin \theta_g \hat{j}^\varphi d\hat{V} \\ &= \bar{R}_0^4 \int_{\mathcal{M}} \Psi^6 \hat{r}_g \sin \theta_g \frac{q^n \lambda}{h\alpha} \hat{\nabla}^\varphi \Phi d\hat{V}. \end{aligned} \quad (106)$$

In the following we will denote a half of the total rest-mass, the ADM mass and the angular momentum by $\bar{M}_0 = \bar{M}_{0,\text{tot}}/2$, $\bar{M} = \bar{M}_{\text{ADM}}/2$ and $\bar{J} = \bar{J}_{\text{tot}}/2$, respectively. In the limit of a large separation, \bar{M}_0 and \bar{M} approach the corresponding values of isolated stars.

We also use the averaged separation d_G which coincides with the separation between mass centers of two component stars in Newtonian limit, namely,

$$\begin{aligned} \bar{d}_G &= \kappa^{-n/2} d_G \\ &= \frac{\bar{R}_0}{\bar{M}_0} \int_{\mathcal{M}} \hat{r}_g \sin \theta_g \cos \varphi_g \frac{q^n \lambda \Psi^6}{h\alpha} d\hat{V}. \end{aligned} \quad (107)$$

B. Test of our new computational method

In this paper we will show the results for $n = 1$ polytropes. Thus we need to specify two parameters to obtain one quasi-equilibrium configuration, i.e. the half of separation \hat{d} and the largest value of $q = q_c$. In order to check how our new computational code works, we have compared our results with (a) those of co-rotating GR binary systems tabulated in [10], and with (b) those of Newtonian irrotational binary systems in Paper I. By the former comparison (a), we can check the gravitational field part of our code for strong gravity regime. For more thorough check, it is desirable to compare the present solutions with some analytic or semi-analytic results. The semi-detached irrotational binary systems with 1PN approximation for $n = 0$ polytropes are analytically solved by Taniguchi [27]. Lombardi, Rasio & Shapiro calculated the irrotational polytropic binary systems by partly including 1PN correction terms [28]. We will compare our results with these works as well as the works done by

| z_A | \hat{d} | q_c | $\bar{\Omega}$ | \bar{R}_0 | \bar{M}_0 | \bar{M} | \bar{J} |
|-------|-----------|--------|----------------|-------------|-------------|-----------|-----------|
| 0.20 | 1.50 | 0.0685 | 0.079 | 1.004 | 0.1118 | 0.10552 | 0.02729 |
| | | | 0.079 | 1.005 | 0.1125 | 0.10619 | 0.02780 |
| 0.00 | 1.00 | 0.0658 | 0.101 | 1.177 | 0.1118 | 0.10551 | 0.02715 |
| | | | 0.101 | 1.176 | 0.1128 | 0.10637 | 0.02760 |
| 0.20 | 1.50 | 0.2450 | 0.168 | 0.646 | 0.1781 | 0.16013 | 0.04948 |
| | | | 0.168 | 0.643 | 0.1801 | 0.16169 | 0.05050 |
| 0.00 | 1.00 | 0.2164 | 0.202 | 0.780 | 0.1781 | 0.16018 | 0.05024 |
| | | | 0.203 | 0.774 | 0.1807 | 0.16227 | 0.05132 |

TABLE II. Comparison between the results of Baumgarte et al. (1997) and those of the present method for co-rotating GR binary systems. The first line of each model corresponds to the result of Baumgarte et al. (1997) and the second line to the present result. The first two models correspond to the system with $(M/R)_\infty = 0.1$ and the latter two models to $(M/R)_\infty = 0.2$ in Baumgarte et al. (1997). $z_A = 0.0$ corresponds to the contact binary system and $z_A = 0.2$ to the semi-detached binary system where $z_A = R_{\text{in}}/R_{\text{out}}$.

other authors who have used the identical formulation but different numerical computational methods in the future.

It is convenient to characterize solutions or sequences by using the total rest mass $M_0 = \text{const}$ or, equivalently, the compactness $(M/R)_\infty$ of an isolated spherical star. In actual computations, we choose a certain value for M_0 and adjust the parameter q_c so that the value of M_0 is kept constant during the iteration.

In Table II, we compare our results for co-rotating binary systems with those in [10]. For these models we have replaced the equations for the fluid part by those for co-rotating fluids. Therefore, the code for the gravitational part has been checked. We set the values of \hat{d} and q_c as same as those in [10] for each model. As shown in Table II, the obtained quantities $\bar{\Omega}$ and \bar{R}_0 which characterize the models for BNS's are in good agreement (relative errors are less than 1%). For integral quantities \bar{M}_0 , \bar{M} and \bar{J} , relative errors are at most 2%.

Next, we compare our results of a quasi-equilibrium sequence of irrotational binary systems in weak gravity with those of Newtonian computations. It is reasonable to assume that the total rest mass is constant throughout the final evolution. Thus the quasi-equilibrium sequence with $M_0 = \text{const}$ mimics the realistic evolution sequence as a result of GW emission. In Figure 2, we compare our present results of the compactness $(M/R)_\infty = 0.001$ with those in Paper I. In this figure, \bar{J} is plotted against the separation \bar{d}_G or $\bar{\Omega}$. Relative errors of \bar{J} at the fixed value of \bar{d}_G or $\bar{\Omega}$ are $\sim 0.5\%$, relative errors of \bar{d}_G at the fixed value of \bar{J} are $\sim 1\%$, and relative errors of $\bar{\Omega}$ at the fixed value of \bar{J} are $\sim 1.7\%$. Therefore, our new code have reproduced the results as those of other computations

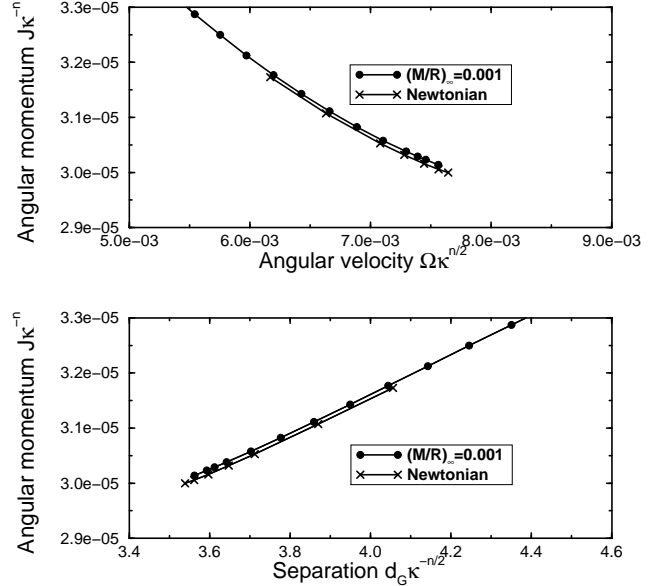


FIG. 2. Comparison between the results of Paper I (Newtonian) and those of the present computation (with compactness $(M/R)_\infty = 0.001$). A quasi-equilibrium sequence of an irrotational BNS system with weak gravity (curve with dots) and that of Newtonian gravity (curve with crosses) are plotted. The angular momentum as a function of the angular velocity (upper panel) and the angular momentum as a function of the separation (lower panel) are shown.

with a reasonable accuracy.

C. Quasi-equilibrium sequences of irrotational binary systems in GR

In Figures 3 and 4 we show contours of GR irrotational BNS systems. As seen from these figures, our numerical method can handle highly deformed configurations of BNS systems and the gravitational field around them. Particularly, in the right panel of Fig. 4, we show the contour for the rest mass density ρ with $(M/R)_\infty = 0.14$. From this figure, we can see that a cusp-like structure appears at the inner edge of stars before two stars contact each other [29]. The cusp is supposed to correspond to the inner Lagrange point (L1 point), where the mass overflow occurs from this point when the separation of two stars becomes smaller than this distance.

In Table III, we tabulate the physical quantities of irrotational BNS systems with the cusp-like structure for various compactness. We also tabulate the dimensionless total angular momentum $J_{\text{tot}}/M_{\text{ADM}}^2$ which is unity for an extreme Kerr black hole. For the co-rotating models [10], $J_{\text{tot}}/M_{\text{ADM}}^2$ becomes unity around $(M/R)_\infty \sim 0.175$. On the other hand, this value for irrotational BNS systems becomes unity around $(M/R)_\infty \sim 0.12$ as shown in Table III. This is a result of the counter rotation with respect

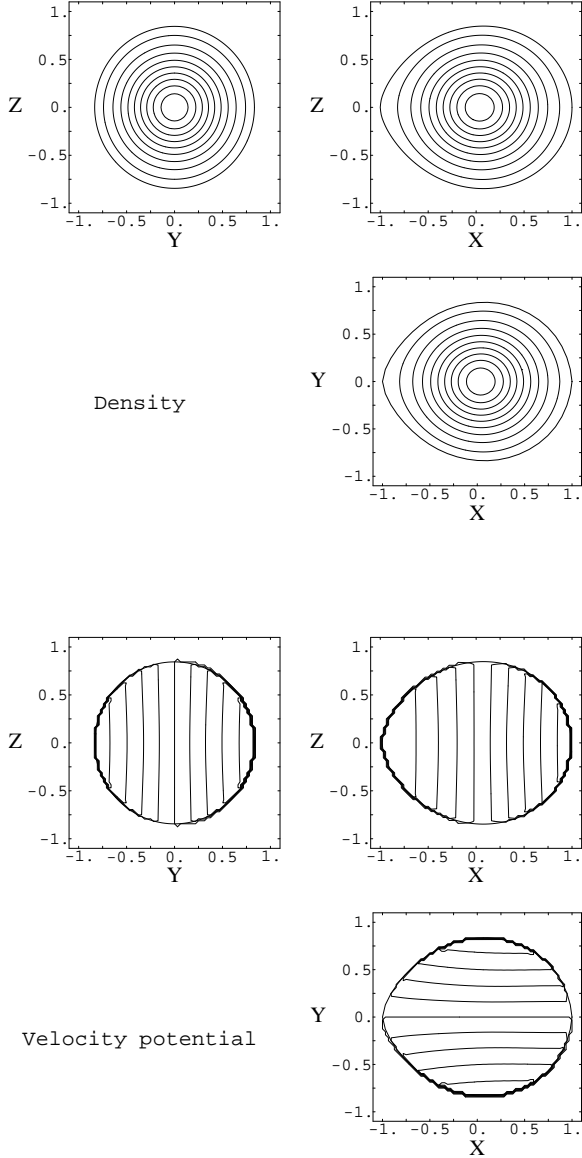


FIG. 3. Structure of a component star of an irrotational BNS system. Contours of the rest mass density ρ distribution (upper three panels) and the velocity potential distribution Φ (lower three panels) are drawn for the model with $(M/R)_\infty = 0.17$ and $\hat{d} = 1.25$. YZ -plane (upper left panel), ZX -plane (upper right) and XY -plane (lower right panel) correspond to the $\varphi_f = 0$ and π plane, the $\varphi_f = \pi/2$ plane, and the $\theta_f = \pi/2$ plane, respectively. Length in figures is normalized by R_0

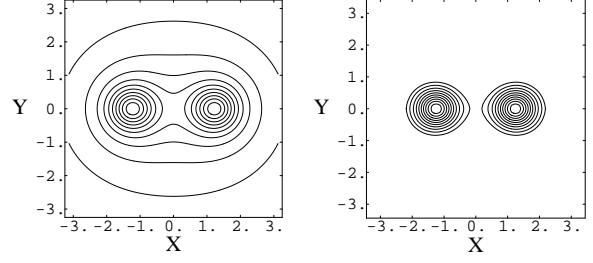


FIG. 4. Contours of the conformal factor Ψ^4 (left panel) and the rest mass density distribution (right panel) for the model with $(M/R)_\infty = 0.14$ and $\hat{d} = 1.25$. Length in figures is normalized by R_0

| $(M/R)_\infty$ | \bar{M}_0 | \bar{M} | $\Omega\bar{M}_0$ | $J_{\text{tot}}/\bar{M}_{\text{ADM}}^2$ | \bar{R}_0 |
|----------------|-------------|-----------|-------------------|---|-------------|
| 0.1 | 0.112 | 0.105 | 0.0110 | 1.08 | 1.07 |
| 0.12 | 0.130 | 0.121 | 0.0148 | 1.01 | 0.979 |
| 0.14 | 0.146 | 0.135 | 0.0192 | 0.963 | 0.899 |
| 0.17 | 0.166 | 0.150 | 0.0271 | 0.911 | 0.783 |

TABLE III. Physical quantities of the irrotational BNS near the configuration with a cusp-like structure (L1 point).

to the orbital motion of each component star. Therefore, after coalescence of two stars due to GW emission, irrotational BNS systems could form a single Kerr black hole with losing much less angular momentum to the environment than co-rotating BNS systems.

In Figures 5, we show the quasi-equilibrium sequences for several values of $(M/R)_\infty$. The binding energy $(\bar{M} - \bar{M}_\infty)/\bar{M}_\infty$ and \bar{J} are plotted against the normalized orbital angular velocity $\Omega\bar{M}_0$. Since each curve is a sequence with constant rest mass \bar{M}_0 , an evolutionary track of a BNS system can be approximated by each curve from the smaller to larger value of $\Omega\bar{M}_0$ as a result of GW emission. The terminal points of curves, i.e. points with the largest $\Omega\bar{M}_0$, roughly correspond to configurations with L1 point. Analogous to Newtonian models as well as GR co-rotating binary systems [30,10], turning points on these curves are expected to correspond to the points where dynamical instability sets in. Our results show that any systems with different values of compactness $(M/R)_\infty$ have no turning points. Therefore irrotational binary configurations with $n = 1$ are thought to be dynamically stable. In other words, at the final inspiraling phase, it is probable that the mass exchange starts earlier than the onset of the orbital motion instability.

V. DISCUSSION AND CONCLUSION

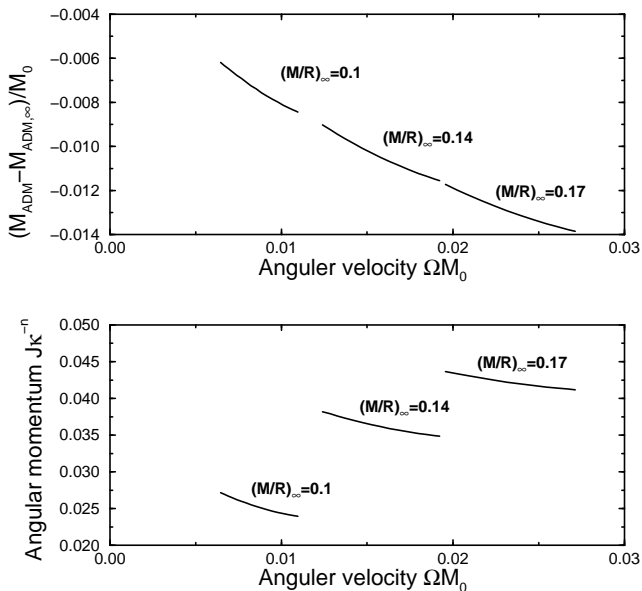


FIG. 5. The binding energy (upper panel) and the angular momentum (lower panel) are plotted against the orbital angular velocity. Each curve corresponds to a $M_0 = \text{const}$ sequence. The value of the compaction $(M/R)_\infty$ of an isolated star is attached to each curve. Cusp-like shape appears for the terminal model with the largest ΩM_0 along each curve.

A. Position of the present numerical method

As mentioned in section II A, there are two different numerical schemes to solve irrotational binary star systems in GR [15,16]. The basic formulation and basic equations are almost the same but numerical schemes are different.

Bonazzola, Gourgoulhon and Marck [15] have used the multi-domain pseudo spectral method. They have introduced several coordinate systems one of which is a fitted coordinate system to the stellar surface. The basic equations which are basically the same as those in this paper are solved by using the pseudo-spectral method on these domain. Although the implementation of numerical method is rather complicate, it produces numerical ‘exact’ solutions with excellent accuracy.

Marronetti, Mathews and Wilson [16] have used the Cartesian coordinate system and a finite difference method on the discretized coordinates to solve the equations which are also the same as ours. This is the standard method which is commonly used in 3D numerical relativity to solve compact binary systems. For instance, it could be advantageous for providing initial data for future 3D simulations of BNS coalescence.

Despite of presence of these two methods, we have presented our new scheme in this paper. There are several reasons for that. First, since quasi-equilibrium states of binary neutron star systems have important meaning in GW investigations, it would be better to get reliable so-

lutions by studying from many directions even if it is the same problem. Second, obtained results from these two schemes seem to be somewhat different. In particular, the behavior of the maximum density during evolution is different as will discussed in the next subsection.

In our solving method, we have used the integral form to solve Poisson type equations. A spherical coordinate system is introduced to implement this Poisson solver. From our experience for numerical computations, it is desirable to use spherical coordinate systems to solve structures of component stars. On the other hand, to solve gravitational field, it is possible to implement Cartesian coordinates and suitable sophisticated Poisson solvers for the coordinates (for instance, multi-grid method, ICCG, and so on). Such implementation could be also useful for preparing initial conditions for numerical simulations as well as checking of the present numerical results.

B. Individual collapse of the irrotational BNS system

The close binary system of irrotational stars has attracted a wide attention because of two reasons. One is that, as mentioned in Section I, it is more probable that such a situation is realized just before coalescence due to GW emission, since viscosity is not strong enough to synchronize the spin of a NS and the orbital motion [3] at this stage. The other reason is that the numerical simulation of irrotational binary systems done by Wilson, Mathews and Marronetti [9] showed the result that the maximum density of the NS increases during the inspiraling due to the GR effect. They proposed a new scenario for the final inspiraling phase of irrotational BNS systems, namely, each component star of a BNS system individually collapses to form a binary black hole system, and after that two black holes would coalesce.

This scenario is debated by many authors (see [15,31] and references therein). The latest numerical computation by Marronetti, Mathews and Wilson [16] shows that the maximum density again increases a few percent for a sequence of models with larger compaction $(M/R)_\infty = 0.19$. On the other hand, the computation by the Meudon numerical relativity group [15] does not show this tendency. In Figure 6, we show our results for the relative change of the maximum energy density $(e_{\text{max}} - e_\infty)/e_\infty$ of a star against the separation \hat{d} . Here $e = \rho(1 + \varepsilon)$, e_{max} is its maximum value and e_∞ is its value in an isolation state which is computed by solving the TOV equation. These are the same sequences as those plotted in Figs. (2) and (5). Because of the numerical error, the value of e_{max} does not tend to e_∞ even when the component stars are detached. (For instance, the value of $(e_{\text{max}} - e_\infty)/e_\infty$ shift about 3% for the case with $(M/R)_\infty = 0.17$). However, this numerical error may not affect the tendency of change for $(e_{\text{max}} - e_\infty)/e_\infty$ along each solution sequences. Our results show that the

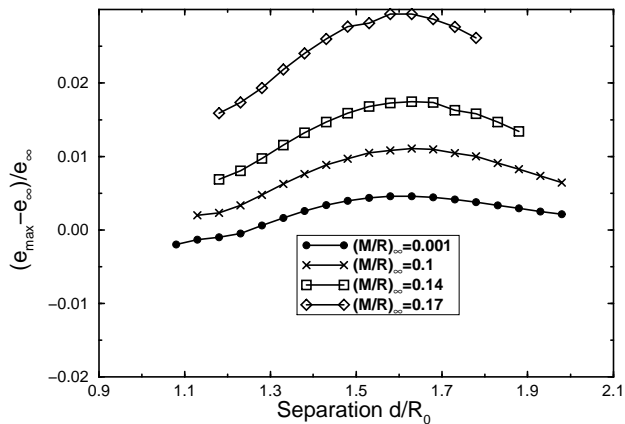


FIG. 6. Relative change of the maximum energy density. Horizontal axis corresponds to the coordinate separation in units of R_0 for each model. The maximum density does not increase substantially as the separation decreases.

energy density changes in the range of 0.5% to 1.5% at most and decreases as the separation decreases. Therefore, we cannot observe the maximum density to increase and hence the tendency of subsequent individual collapse in the present computation. The reason of the difference could be as follows. In [16], they approximate the surface where boundary condition Eq. (56) is imposed by a sphere (but not the actual stellar surface) and expand Eq. (78) up to $l \leq 4$ which could be not enough, since it is known that the dependence of the maximum density on the separation is of $\mathcal{O}(1/r^6)$ for the Newtonian case. We also note that relative changes of order of a few percent for local quantities are smaller than the estimated errors which are included in the conformally flat approximation. On the other hand our computation becomes less accurate for the systems with larger separations since the discretized spherical coordinate grid to compute metric functions becomes coarser.

C. Future prospects

It is important to compute quasi-equilibrium configurations to connect the inspiraling phase, where the perturbative expansion technique can be applied, to the merging phase, where fully dynamical computations are required. Such computations are also useful since the quasi-equilibrium solutions give accurate and appropriate initial conditions for simulations of BNS coalescence [6].

In our formulation we have used so called the Wilson–Mathews formulation to treat the GR effect. However it is known that this approach is exact only up to 1PN order for binary systems in terms of the post-Newtonian terminology, although 2PN or higher order corrections should

be included to express realistic BNS systems. Asada and Shibata [14] have formulated Einstein equations to express BNS systems exactly up to 2PN order. Implementing their equations into numerical computations may be one of possible ways to construct quasi-equilibrium BNS systems, although it is required to solve 29 elliptic PDEs simultaneously for the gravitational field. Recently, Usui, Uryū and Eriguchi [32] have developed a new scheme to compute quasi-equilibrium configurations by using a quite different metric from that of the Wilson–Mathews formulation. It would be interesting to compare results from their method with our present results. Also several authors have constructed a formulation for so called ‘intermediate binary black hole’ (IBBH) states [33]. This formulation could be applicable to quasi-equilibrium states of BNS systems too.

D. Summary and conclusion

We have constructed a numerical method to compute quasi-equilibrium states of irrotational binary systems composed of compressible gaseous stars in general relativity. The new numerical method is based on the standard finite difference method and therefore implementation is rather simple and straightforward. We have used two coordinate systems for computation, one for the gravitational field variables and the other for the fluid variables. Physical quantities are interpolated from one to the other. We have shown that such a procedure works well by actual numerical computations of irrotational BNS systems in GR.

The basic equation for the irrotational flow becomes an elliptic PDE with a Neumann type boundary condition at the stellar surface. For the treatment of general relativistic gravity, we have used the Wilson–Mathews formulation. In this formulation, the basic equations are again expressed by a system of elliptic PDEs. We have developed a method to solve these PDEs. We have checked and compared our solutions with those of previous numerical computations available. Those results of independent computations coincide well with each other.

We have succeeded in computing quasi-equilibrium sequences of irrotational BNS systems in GR. As the Newtonian case, the BNS has been found to be dynamically stable during the inspiraling stage until Roche lobe overflow starts at L1 point. The quasi-equilibrium sequences also suggest that the substantial increase of the maximum energy density does not occur during the inspiraling phase as a result of GW emission. Further investigations of numerical computations and implementation of various realistic EOS’s and/or realistic formulation of GR gravity are interesting and inevitable issues for theoretical predictions of GW signals supposed to be detected by the interferometric GW detectors in the next century.

ACKNOWLEDGMENTS

The author (KU) would like to thank Prof. J. C. Miller for discussion and continuous encouragement. He also would like to thank Profs. D. W. Sciama and A. Lanza, for his warm hospitality at SISSA and ICTP. The part of the numerical computation was carried out at the Astronomical Data Analysis Center of the National Astronomical Observatory, Japan.

-
- [1] A. Abramovici et al., *Science* **256**, 325 (1992); C. Bradaschia et al., *Nucl. Instrum. and Methods* **A289**, 518 (1990); J. Hough, in *Proceedings of the Sixth Marcel Grossmann Meeting*, edited by H. Sato and T. Nakamura (World Scientific, Singapore, 1992), p.192; K. Kuroda et al., in *Proceedings of the international conference on gravitational waves: Sources and Detectors*, edited by I. Ciufolini and F. Fidecard (World Scientific, Singapore, 1997), p.100.
 - [2] Edited by T. Nakamura, *Perturbative and Numerical Approaches to Gravitational Waves*, *Prog. Theor. Phys. Suppl.*, **128**, (1997) ; F. A. Rasio and S. L. Shapiro, *Class. Quant. Grav.*, in press, (gr-qc/9902019).
 - [3] C. S. Kochanek, *ApJ* **398**, 234 (1992); L. Bildsten and C. Cutler, *ApJ* **400**, 175 (1992).
 - [4] K. Oohara and T. Nakamura, in *Relativistic gravitation and gravitational radiation*, edited by J.-P. Lasota and J.-A. Marck (Cambridge University Press, Cambridge, 199), 309; T. Nakamura and K. Oohara, in *Numerical Astrophysics*, edited by S. Miyama (1998) (gr-qc/9812054).
 - [5] E. Seidel and W. M. Suen, Submitted to *J. Comput. Appl. Math.*, (1999).
 - [6] M. Shibata, *Prog. Theor. Phys.* **101**, 251 (1999); M. Shibata, *Prog. Theor. Phys.* **101**, 1199 (1999); M. Shibata, *PRD*, in press (1999) (gr-qc/9908027).
 - [7] S. L. Shapiro and S. A. Teukolsky, *Black Holes, White Dwarfs and Neutron Stars*, (Wiley, New York, 1983).
 - [8] K. Uryū and Y. Eriguchi, *MNRAS* **296**, L1 (1998a), (astro-ph/9712203); K. Uryū and Y. Eriguchi, *ApJS* **118**, 563 (1998b) Paper I, (astro-ph/9808118); K. Uryū and Y. Eriguchi, *MNRAS* **303**, 329 (1999), (astro-ph/9808120).
 - [9] J. R. Wilson and G. J. Mathews, *Phys. Rev. Lett.* **75**, 4161 (1995); J. R. Wilson, G. A. Mathews and P. Marronetti, *Phys. Rev. D* **54**, 1317 (1996).
 - [10] T. W. Baumgarte, G. B. Cook, M. A. Scheel, S. L. Shapiro and S. A. Teukolsky, *Phys. Rev. D* **57**, 7299 (1998).
 - [11] M. Shibata, *Phys. Rev. D* **58**, 024012 (1998).
 - [12] S. A. Teukolsky, *ApJ* **504**, 442 (1998).
 - [13] S. Bonazzola, E. Gourgoulhon and J.-A. Marck, *Phys. Rev. D* **56**, 7740 (1997); H. Asada, *Phys. Rev. D* **57**, 7292 (1998).
 - [14] H. Asada and M. Shibata, *Phys. Rev. D* **54**, 4944 (1996); M. Shibata, *Phys. Rev. D* **55**, 6019 (1997).
 - [15] S. Bonazzola, E. Gourgoulhon and J.-A. Marck, to be published in the proceedings of 19th Texas Symposium on Relativistic Astrophysics: Texas in Paris, Paris, France (1998); S. Bonazzola, E. Gourgoulhon and J.-A. Marck, *Phys. Rev. Lett.* **82**, 892 (1999).
 - [16] P. Marronetti, G. J. Mathews and J. R. Wilson, to be published in the proceedings of 19th Texas Symposium on Relativistic Astrophysics: Texas in Paris, Paris, France (1998); P. Marronetti, G. J. Mathews and J. R. Wilson, to be published in *Phys. Rev. D* (1999).
 - [17] M. Shibata and T. Nakamura, *Phys. Rev. D* **52**, 5428 (1995).
 - [18] A. H. Taub, *Arch. Ratl. Mech. Anal.* **3**, 312 (1959); B. Carter, in *Active Galactic Nuclei*, edited by C. Hazard and S. Mitton (Cambridge University Press, Cambridge, 1979), p.273; V. Moncrief, *ApJ* **235**, 1038 (1980).
 - [19] I. Hachisu, *ApJS* **62**, 461 (1986).
 - [20] H. Komatsu, Y. Eriguchi, I. Hachisu, *MNRAS* **237**, 355 (1989).
 - [21] J. P. Ostriker, J. W.-K. Mark, *ApJ* **151**, 1075 (1968).
 - [22] Instead of this choice, we also set $q = q_c$ at the coordinate center of the star, that is $r_f^* = 0$, in some case. The results do not change by this different choice.
 - [23] G. B. Cook, S. L. Shapiro and S. A. Teukolsky, *ApJ* **398**, 203 (1992).
 - [24] S. Bonazzola, E. Gourgoulhon and J.-A. Marck, *Phys. Rev. D* **58**, 104020 (1998).
 - [25] T. Nozawa, N. Stergioulas, E. Gourgoulhon, Y. Eriguchi, *A&AS* **132**, 431 (1998).
 - [26] J. M. Bowen and J. W. York, Jr., *Phys. Rev. D* **21**, 2047 (1980).
 - [27] K. Taniguchi, *Prog. Theor. Phys.* **101**, 283 (1999); K. Taniguchi, PhD thesis, Kyoto University, (1999).
 - [28] J. C. Lombardi, Jr., F. A. Rasio and S. L. Shapiro, *Phys. Rev. D* **56**, 3416 (1997).
 - [29] The cusp is formed before the two stars contact each other even for Newtonian equal mass BNS's with polytropic EOS, because of the non-synchronized rotation of the stars. This fact was overlooked in the previous paper by the present authors (Paper I). Although the cusp forms just before the contact phase, changes of numerical results are to within less than 2% and statements in [8] are not affected. The authors thank Dr. E. Gourgoulhon for pointing this out.
 - [30] D. Lai, F. A. Rasio and S. L. Shapiro, *ApJS* **88**, 205 (1993); T. W. Baumgarte, G. B. Cook, M. A. Scheel, S. L. Shapiro and S. A. Teukolsky, *Phys. Rev. D* **57**, 6181 (1998).
 - [31] P. Marronetti, G. J. Mathews and J. R. Wilson, *Phys. Rev. D* **58**, 043003 (1998).
 - [32] F. Usui, K. Uryū and Y. Eriguchi, *Phys. Rev. D*, in press (1999).
 - [33] P. R. Brady, J. D.E. Creighton and K. S. Thorne, *Phys. Rev. D* **58**, 061501 (1998); K. S. Thorne, Submitted to *Phys. Rev. D* (1998), (gr-qc/9808024).